ISSN 2176-5480

22nd International Congress of Mechanical Engineering (COBEM 2013)
November 3-7, 2013, Ribeirão Preto, SP, Brazil

DIFFUSION-BASED LIMITERS FOR DISCONTINUOUS GALERKIN METHODS - PART I: ONE-DIMENSIONAL EQUATIONS

Rodrigo Costa Moura
Rodrigo Castellari Affonso
André Fernando de Castro da Silva
Marcos Aurélio Ortega
Technological Institute of Aeronautics - ITA, São José dos Campos, Brazil
moura@ita.br, rodrigoaffonso@aluno.ita.br, andref@ita.br, ortega@ita.br

Abstract. *Within the context of high-order accurate methods, the treatment of shock waves in the numerical solution of non-linear hyperbolic equations is still a highly relevant field of research. In the last years, limiting techniques traditionally used with low-order schemes have been successfully adapted and extended for high-order methods. The same can be said about artificial viscosity approaches; specifically, for the Discontinuous Galerkin (DG) method, recent works based on such concept brought to the DG formulation the so called sub-cell shock resolution, namely, the capability of representing shocks within a single mesh element. Typically, however, opting for artificial viscosity techniques in the DG context requires the additional use of specific schemes to account for the artificial diffusion terms. Moreover, the introduction of an elliptic bias to originally hyperbolic equations severely restrains the (explicit) time-stepping stability envelope. The choice for limiters does bypass such difficulties but, on the other hand, usually comes with drawbacks such as implementation complexity, residue convergence problems and, normally, lack of sub-cell resolution. This study presents a new type of shock capturing operator which practically does not suffer from any of the aforementioned disadvantages. In summary, it works as a filter damping high-frequency modes, but is based on the concept of artificial viscosity, being however applied as a limiter. In its final form, such diffusion-based limiter is implemented in an extremely simple way. The operator is also relatively inexpensive and yet capable of providing results of surprising quality. Numerical tests demonstrate fine sub-cell resolution as well as local accuracy scaling with h/p.*

Keywords: *Shock Treatment, Discontinuous Galerkin Method, High-order Schemes, CFD.*

1. INTRODUCTION

Shock waves are well known physical structures that exist as a result of the compressibility of fluids, specially the air. The importance of shock waves in engineering becomes evident in the aerospace context, where compressible flows interact with vehicles traveling at supersonic speeds (Anderson, 2002). Therefore, minding CFD simulation and subsequent design, the correct treatment of shock waves is of paramount importance when it comes to the numerical solution of fluid flow equations.

Within the last two decades, the so called high-order methods (Ekaterinaris, 2005; Wang, 2007) are emerging in order to properly address flow problems which particularly require highly accurate treatment, such as wave propagation for aeroacoustics, vortex-dominated flows, turbulence simulation and also flows with complex shock interactions (Lê *et al.*, 2011). However, one of the issues difficulting a wider adoption of high-order methods amongst CFD practitioners is the recognized need for robust and accurate shock capturing techniques suited for those methods (Vincent and Jameson, 2011; Wang *et al.*, 2013). The numerical treatment of flow discontinuities is addressed since several decades ago (von Neumann and Richtmyer, 1950), but can still be considered a highly relevant field of research, specially in the context of high-order schemes.

The present article focus on a modern but already popular high-order method known as Discontinuous Galerkin (DG) (Cockburn *et al.*, 2000; Hesthaven and Warburton, 2008). The reader is referred to the work of Moura (2012) for a detailed introduction to the method. Concerning the treatment of shock waves, a variety of algorithms have been proposed specifically for the DG formulation in the last years. For instance, different limiting techniques have been adapted and extended for the DG scheme (Cockburn and Shu, 2001; Qiu and Shu, 2005; Krivodonova, 2007; Kuzmin, 2010). The same can be said about artificial viscosity approaches (Persson and Peraire, 2006; Barter and Darmofal, 2007, 2010; Atkins and Pampell, 2011); its worth mentioning that such viscous approaches brought to the DG formulation the so called sub-cell shock resolution, namely, the distinctive capability of representing shocks within a single mesh element.

Working, however, with shock-capturing techniques based on artificial viscosity for the solution of hyperbolic equations (such as the Euler equations of gas dynamics) in a DG context requires the additional use of specific schemes to account for the artificial diffusion terms (Arnold *et al.*, 2002). Furthermore, the introduction of an elliptic bias to originally hyperbolic equations severely restrains the time-stepping stability envelope (Klockner *et al.*, 2011) when using explicit time discretizations. The choice for limiters does bypass such difficulties but, on the other hand, usually comes with

ISSN 2176-5480

drawbacks such as implementation complexity, residue convergence problems and, normally, lack of sub-cell resolution (Vincent and Jameson, 2011; Wang *et al.*, 2013).

This article presents a new type of shock-capturing operator which practically does not suffer from any of the aforementioned problems. In resume, it works as a filter damping high-frequency modes, but is based on the concept of artificial viscosity, being however applied as a limiter. In its final form, such diffusion-based limiter is implemented in an extremely simple way. The operator is also relatively inexpensive and yet capable of providing results of surprising quality. Numerical tests demonstrate fine sub-cell resolution as well as local accuracy scaling with h/p (where h is the local mesh size and p is the degree of the polynomial expansion representing the solution), i.e. the same local accuracy obtained with modern artificial viscosity approaches (Persson and Peraire, 2006; Barter and Darmofal, 2010).

The present study is organized in the following way. Section 2 introduces the reader to the DG discretization for convection-diffusion problems in one dimension. It also discuss the idea behind shock-capturing artificial viscosity approaches and how they affect the (explicit) time-marching stability envelope. In section 3 the diffusion-based limiter is presented, both in terms of theory and implementation. Numerical tests are addressed in section 4, where the (inviscid) Burgers' equation is used to evaluate the operator local order of accuracy. Moreover, a specific form of the one-dimensional Euler equations is solved to present the reader some of the fine results one can expect for "practical" problems. At last, concluding remarks are given in section 5 along with future research possibilities.

2. THE DISCONTINUOUS GALERKIN FORMULATION

2.1 Discretizing the model equation

A generalized convection-diffusion (scalar) equation is here adopted as model equation for the DG formulation. Being Ω the one-dimensional domain of interest and given suited initial and boundary conditions, one have

$$\frac{\partial u}{\partial t} + \frac{\partial f}{\partial x} = \frac{\partial f_v}{\partial x} \quad \text{in } \Omega \,, \tag{1}$$

where $f = f(u)$ and $f_v = f_v(u, \partial u/\partial x)$ are, in that order, the inviscid and viscous flux functions. Traditionally, to solve Eq. (1), the second-order PDE must be split into a system of two first-order PDEs, namely,

$$\frac{\partial u}{\partial t} + \frac{\partial}{\partial x}\left(f(u) - f_v(u, g)\right) = 0 \,, \tag{2}$$

$$g - \frac{\partial u}{\partial x} = 0 \,, \tag{3}$$

by which the gradient function $g(x)$ is introduced. At this point, one must proceed with the hp discretizations.

By h discretization, one means partitioning the domain Ω into non-overlapping elements Ω_e such that $\Omega = \bigcup_e \Omega_e$. The p discretization consists of representing the (approximated) numerical solution $u(x,t)$ within each element through the sum of local basis functions ϕ_i, normally polynomials of degree equal or less than P, weighted by coefficients c_i to be adjusted. It must be empathized that while the coefficients c_i are time-dependent, the modal functions ϕ_i are not, being however pre-defined in the standard domain $\Omega_{st} = [-1, 1]$. In mathematical terms,

$$u(x,t)|_{\Omega_e} \cong \sum_{i=0}^{P} c_i^{(e)}(t)\, \phi_i(\xi) \,, \tag{4}$$

where the variables $\xi \in \Omega_{st}$ and $x \in \Omega_e$ are related by linear mappings given by

$$x(\xi) = \frac{1-\xi}{2}\, x_e^{\ominus} + \frac{1+\xi}{2}\, x_e^{\oplus} \,, \quad \xi \in \Omega_{st} = [-1, 1] \,, \tag{5}$$

$$\xi(x) = -1 + 2\,\frac{x - x_e^{\ominus}}{x_e^{\oplus} - x_e^{\ominus}} \,, \quad x \in \Omega_e = [x_e^{\ominus}, x_e^{\oplus}] \,, \tag{6}$$

in which $x_e^{\ominus}$ and $x_e^{\oplus}$ are the left and right coordinates of element Ω_e, respectively.

Here, the Legendre polynomials are chosen to generate the basis functions, since an orthogonal space of functions can be spanned by this polynomial family. The Legendre polynomial of degree k can be obtained as a particular case of Rodrigue's formula (Askey, 2005), being given by

$$\mathcal{P}_k(\xi) = \frac{(-1)^k}{2^k k!}\frac{d^k}{d\xi^k}\left[(1-\xi^2)^k\right] \,, \quad \xi \in \Omega_{st} \,. \tag{7}$$

ISSN 2176-5480

In a numerical context, however, such polynomials (and its derivatives) are evaluated recursively through the following expressions, already simplified from the textbook of Karniadakis and Sherwin (2005):

$$(k+1)\,\mathcal{P}_{k+1}(\xi) = (2k+1)\,\xi\,\mathcal{P}_k(\xi) - k\,\mathcal{P}_{k-1}(\xi)\,, \tag{8}$$

$$(1-\xi^2)\,\frac{d}{d\xi}\mathcal{P}_k(\xi) = -k\,\xi\,\mathcal{P}_k(\xi) + k\,\mathcal{P}_{k-1}(\xi)\,, \tag{9}$$

where the initial values needed for the recursive process can be calculated analytically from Eq. (7).

The Legendre polynomials are said to be orthogonal in Ω_{st} in the sense that

$$\int_{\Omega_{st}} \mathcal{P}_i(\xi)\mathcal{P}_j(\xi)\,d\xi = \frac{\delta_{ij}}{i+1/2}\,, \tag{10}$$

where δ_{ij} is the Kronecker delta, being one if $i=j$ and zero otherwise. Therefore, it is handy to normalize them in order to use an orthonormal set of basis functions ϕ_i, namely,

$$\phi_i(\xi) = \sqrt{i+1/2}\,\mathcal{P}_i(\xi)\,, \tag{11}$$

such that

$$\int_{\Omega_{st}} \phi_i(\xi)\phi_j(\xi)\,d\xi = \delta_{ij}\,. \tag{12}$$

Now, returning to Eqs. (2) and (3), one must follow the (standard) Galerkin method so as to make the projection of both PDEs to vanish within the approximating element-wise polynomial space of functions. This condition must hold locally for each element Ω_e. Working first with Eq. (2), the procedure consists of enforcing

$$\int_{\Omega_e} \phi_j \left[\frac{\partial u}{\partial t} + \frac{\partial}{\partial x}(f - f_v)\right] dx = 0 \quad \text{for } j = 0, ..., P\,. \tag{13}$$

Such set of equations can be translated into corresponding expressions for the coefficients $c_i^{(e)}$, once

$$\int_{\Omega_e} \phi_j \frac{\partial u}{\partial t}\,dx = \int_{\Omega_e} \phi_j \left(\sum_{i=0}^{P} \frac{dc_i}{dt}\phi_i\right) dx = \sum_{i=0}^{P} \left(\frac{dc_i}{dt}\int_{\Omega_e} \phi_j\phi_i\,dx\right) = J_e\frac{dc_j}{dt}\,, \tag{14}$$

since, by Eq. (12),

$$\int_{\Omega_e} \phi_i\phi_j\,dx = J_e\int_{\Omega_{st}} \phi_i\phi_j\,d\xi = J_e\,\delta_{ij}\,, \tag{15}$$

where J_e is the transformation Jacobian associated with Ω_e, which, through Eq. (5), is given by

$$J_e = \frac{dx}{d\xi} = \frac{x_e^{\oplus} - x_e^{\ominus}}{2}\,. \tag{16}$$

The remaining terms related to Eq. (13) can be worked out by noticing that

$$\phi_j\frac{\partial}{\partial x}(f - f_v) = \frac{\partial}{\partial x}\left[(f - f_v)\phi_j\right] - (f - f_v)\frac{\partial \phi_j}{\partial x}\,. \tag{17}$$

Communication between adjacent elements is now introduced in the formulation by making

$$\int_{\Omega_e} \phi_j\frac{\partial}{\partial x}(f - f_v)\,dx \cong \Big[(\tilde{f} - \tilde{f}_v)\phi_j\Big]_{\Omega_e^{\ominus}}^{\Omega_e^{\oplus}} - \int_{\Omega_e} (f - f_v)\frac{\partial \phi_j}{\partial x}\,dx\,, \tag{18}$$

where $\tilde{f} = \tilde{f}(u_L, u_R)$ and $\tilde{f}_v = \tilde{f}_v(u_L, g_L, u_R, g_R)$ are numerical fluxes (to be defined) based on the solution values at the left side (L) and at the right side (R) of the boundaries $\Omega_e^{\ominus}$ and $\Omega_e^{\oplus}$, since the global solution is allowed to be discontinuous and therefore double-valued at interfaces.

Using Eqs. (14) and (18) in Eq. (13) yields

$$J_e\frac{dc_i}{dt} = \int_{\Omega_e} (f - f_v)\frac{\partial \phi_i}{\partial x}\,dx - \Big[(\tilde{f} - \tilde{f}_v)\phi_i\Big]_{\Omega_e^{\ominus}}^{\Omega_e^{\oplus}} \quad \text{for } i = 0, ..., P\,. \tag{19}$$

ISSN 2176-5480

Working now with Eq. (3), the same procedure must be applied. In order to do that, the gradient function $g(x)$ can be written within each element Ω_e as

$$g(x,t)|_{\Omega_e} \cong \sum_{i=0}^{P} \gamma_i^{(e)}(t)\,\phi_i(\xi)\;, \tag{20}$$

where the coefficients γ_i rely upon the solution $u(x,t)$, being obtained through the set of equations

$$\int_{\Omega_e} \phi_j \left(g - \frac{\partial u}{\partial x}\right) dx = 0 \quad \text{for } j = 0, ..., P\;. \tag{21}$$

Such expressions can be worked out by noticing that

$$\phi_j \frac{\partial u}{\partial x} = \frac{\partial}{\partial x}(u\phi_j) - u\frac{\partial \phi_j}{\partial x}\;, \tag{22}$$

which can be used to yield

$$J_e\gamma_i = [\tilde{u}\,\phi_i]_{\Omega_e^\ominus}^{\Omega_e^\oplus} - \int_{\Omega_e} u\frac{\partial \phi_i}{\partial x}\,dx \quad \text{for } i = 0, ..., P\;, \tag{23}$$

where $\tilde{u} = \tilde{u}(u_L, u_R)$ is a numerical average (to be defined) which further increases communication across boundaries and is fundamental to the stability of the formulation.

In summary, at each time instant, the numerical solution $u(x,t)$ is used to obtain $g(x,t)$ via Eqs. (20) and (23), so that the flux functions $f(u)$ and $f_v(u,g)$ can be evaluated and used in Eq. (19), yielding dc_i/dt by which the numerical solution can be calculated at the next time step through the application of time discretization techniques. To close the formulation, the numerical fluxes $\tilde{f}$ and $\tilde{f}_v$, as well as the numerical average $\tilde{u}$, must be discussed and defined.

A variety of formulas for the numerical fluxes are available in the literature (Karniadakis and Sherwin, 2005). For the sake of simplicity, two well-known techniques are here adopted. For the inviscid numerical flux $\tilde{f}$, the Lax-Friedrichs formula (Rider and Lowrie, 2002) is employed:

$$\tilde{f}(u_L, u_R) = \frac{1}{2}\left(f(u_L) + f(u_R)\right) - \frac{|\tilde{\lambda}|}{2}\left(u_R - u_L\right)\;, \tag{24}$$

where, as usual, u_L and u_R are the solution values respectively taken from the left and from the right side of the interface in which the flux is being evaluated. For instance, at the interface $x_e^\oplus = x_{e+1}^\ominus$ shared by elements $\Omega_e = [x_e^\ominus, x_e^\oplus]$ and $\Omega_{e+1} = [x_{e+1}^\ominus, x_{e+1}^\oplus]$, they are given by

$$u_L = u^{(e)}(x_e^\oplus) = \sum_{i=0}^{P} c_i^{(e)}\phi_i(+1) = \sum_{i=0}^{P} c_i^{(e)}\phi_i^\oplus\;, \tag{25}$$

$$u_R = u^{(e+1)}(x_{e+1}^\ominus) = \sum_{i=0}^{P} c_i^{(e+1)}\phi_i(-1) = \sum_{i=0}^{P} c_i^{(e+1)}\phi_i^\ominus\;. \tag{26}$$

The value of $\tilde{\lambda}$ corresponds to the eigenvalue related to the inviscid flux function ($\lambda = \partial f/\partial u$) calculated in some mean value of the solution at the considered interface. For the scalar case, the simple average is a valid choice:

$$\tilde{\lambda} = \lambda\left((u_L + u_R)/2\right)\;. \tag{27}$$

For the viscous terms $\tilde{f}_v$ and $\tilde{u}$, the BR2 scheme (Bassi *et al.*, 1997; Brezzi *et al.*, 2000) is here adopted, in which

$$\tilde{u} = \frac{1}{2}\left(u_L + u_R\right)\;, \tag{28}$$

$$\tilde{f}_v(u_L, g_L, u_R, g_R) = \frac{1}{2}\left(f_v(u_L, g_L^\star) + f_v(u_R, g_R^\star)\right)\;, \tag{29}$$

where $g_L^\star$ and $g_R^\star$ are modified gradient functions at the left and right sides of the interface, which for the basis functions here adopted, are given by

$$g_L^\star = \left[\frac{\partial u}{\partial x}\right]_L + \frac{\eta}{2J_L}(u_R - u_L)\sum_{i=0}^{P}(\phi_i^\oplus)^2\;, \tag{30}$$

ISSN 2176-5480

$$g_R^\star = \left[\frac{\partial u}{\partial x}\right]_R + \frac{\eta}{2J_R}(u_R - u_L)\sum_{i=0}^{P}(\phi_i^\ominus)^2 \,, \tag{31}$$

in which η is a stabilization parameter that can be fixed as $\eta = 3$ for the one-dimensional case, J_L and J_R, recall Eq. (16), are the Jacobians of the elements sharing the considered interface from the left and right sides, and the values of $[\partial u/\partial x]_L$ and $[\partial u/\partial x]_R$ are obtained directly by the expressions

$$\left[\frac{\partial u}{\partial x}\right]_L = \left[\frac{\partial}{\partial x}\sum_{i=0}^{P} c_i\phi_i\right]_L = \frac{1}{J_L}\left[\sum_{i=0}^{P} c_i\frac{\partial \phi_i}{\partial \xi}\right]_L = \frac{1}{J_L}\sum_{i=0}^{P} c_i^L \partial_\xi \phi_i^\oplus \,, \tag{32}$$

$$\left[\frac{\partial u}{\partial x}\right]_R = \left[\frac{\partial}{\partial x}\sum_{i=0}^{P} c_i\phi_i\right]_R = \frac{1}{J_R}\left[\sum_{i=0}^{P} c_i\frac{\partial \phi_i}{\partial \xi}\right]_R = \frac{1}{J_R}\sum_{i=0}^{P} c_i^R \partial_\xi \phi_i^\ominus \,. \tag{33}$$

2.2 Treating shocks

The sub-cell shock resolution capability of the DG formulation was first recognized through the work of Persson and Peraire (2006), where a shock capturing operator based on the concept of artificial viscosity was proposed. The idea of the model is to solve the equations of interest with the inclusion of a diffusion term whose magnitude becomes non-zero in the vicinity of discontinuities. For instance, in the case of purely hyperbolic problems, a modified PDE must be used, similar to Eq. (1), where its right-hand side term would represent the artificial diffusion, such that

$$f_v = \epsilon(u)\frac{\partial u}{\partial x} \,, \tag{34}$$

where $\epsilon(u)$ is the viscosity magnitude.

Without proper treatment, Gibbs-like oscillations are known to appear in the presence of shocks, degrading the solution accuracy and possibly causing the simulation to diverge. In the model here considered, an element-wise constant viscosity is used, where the magnitude of ϵ is triggered by the activation of an oscillation sensor, or, more specifically, by a sensor that estimates the solution's lack of resolution. When using orthonormal basis functions, the sensor in question is given, within each element, by

$$\sigma = \frac{c_P^2}{c_0^2 + ... + c_P^2} \,. \tag{35}$$

After calculating σ, the viscosity ϵ is introduced gradually by means of a smooth switching, namely,

$$\epsilon = \begin{cases} 0 & \text{if } \; s < s_o - \kappa \,, \\ \frac{1}{2}\,\epsilon_o\left[1 + \sin\frac{\pi(s - s_o)}{2\kappa}\right] & \text{if } \; s_o - \kappa \leq s \leq s_o + \kappa \,, \\ \epsilon_o & \text{if } \; s > s_o + \kappa \,, \end{cases} \tag{36}$$

where $s = \log_{10}\sigma$, $s_o = -(A + B\log_{10} P)$ and $\epsilon_o = Ch/P$, being h the size of the considered element. Typical values of the model parameters are $A \cong 4$, $B \cong 4$, $C \cong 1/2$ and $\kappa \cong 1/2$, but they are strongly dependent on the particular problems being simulated and may adjusted to furnish optimal results. Also, regarding numerical implementation, it is advisable to add a small constant ($\cong 10^{-10}$) to the value of σ when calculating $s = \log_{10}\sigma$ in order to avoid the divergence of the logarithmic function in the limit of a zero argument (away from discontinuities).

When using viscosity-based shock capturing approaches, discontinuities are turned into continuous gradient layers of length proportional to the viscosity magnitude (von Neumann and Richtmyer, 1950). When artificial diffusion is applied in a DG context, the intention is to spread discontinuities just to the extent where the approximating space is able to resolve shock transitions well, without spurious oscillations. In general, the resolution provided by polynomial functions in a hp discretization scales with $\delta \sim h/p$. In other words, when using a viscosity of magnitude $O(h/p)$, a gradient layer of thickness δ can be adequately represented by a polynomial space of degree p in a mesh of local size h.

The nominal order of accuracy of the DG method for smooth solutions is $P + 1/2$ (Johnson and Pitkaranta, 1986; Richter, 1992). Such error estimates were obtained for simple equations (scalar, linear) and rely upon somewhat restrictive hypothesis. Fortunately, however, order $P + 1$ is often verified even for the complete Navier-Stokes equations in three dimensions, see for instance the cases analyzed in the work of Nogueira *et al.* (2010). On the other hand, in the vicinity of shocks, the accuracy is typically reduced to first order. When using the artificial viscosity model here considered, the error level observed near shocks is compatible with the magnitude of the artificial term introduced on the original PDE, namely, $O(h/p)$, which is normally much better than "plain" first order, $O(h)$, but still far from the usual order of accuracy expected at smooth regions, $O(h^{p+1})$.

ISSN 2176-5480

2.3 Time step reduction

In the simulation of hyperbolic equations, the employment of explicit time discretizations is not only simple but also efficient. When dealing with steady-state problems, the use of local time-stepping techniques is advisable in order to improve the residue convergence rate to the desired solution. Within the DG context, the CFL-based formula (Toulorge and Desmet, 2011) for the time step is given by

$$\Delta t = \frac{h\,\mathrm{CFL}}{(2P+1)|\lambda|}\,, \tag{37}$$

in which h is the local mesh size, λ is the average wave speed within the considered element and CFL is the prescribed Courant-Friedrichs-Lewy number, typically of order one.

For simulations where artificial viscosity models are employed, the time-step stability limits are greatly reduced (for explicit time-marching). The adaptation of the local time-step formula consists of dividing the expression in Eq. (37) by a viscous factor (Klockner *et al.*, 2011) which can be written as

$$v_f = \sqrt{1 + \left(\frac{2P+1}{h}\frac{\epsilon}{|\lambda|}\right)^2}\,, \tag{38}$$

where ϵ is the local viscosity magnitude. It is important to highlight that v_f can be much greater than one, specially for higher-order simulations. This is why the choice for artificial viscosity approaches can be significantly worse than using limiting techniques if one wants to avoid implicit time discretizations.

3. THE DIFFUSION-BASED LIMITER

3.1 Solving the diffusion PDE

The idea behind the limiting technique here proposed consists in applying the diffusion equation as a filtering operator at troubled elements. The oscillating local expansion is taken as initial condition in the solution of the classical diffusion PDE, with suitable boundary conditions prescribed at the edges of the troubled element. During the diffusion process the operator works as a filter damping high-frequency modes of the expansion. This idea was borrowed from the field of image processing, where a similar technique is used to smooth out noisy figure-related data, see for instance the work of Wu *et al.* (2008).

The diffusion equation, also known as the heat equation, is given by

$$\frac{\partial u}{\partial t} = \epsilon\,\frac{\partial^2 u}{\partial x^2}\,, \tag{39}$$

where the element-wise artificial viscosity ϵ is here taken as diffusivity constant. In order to apply the DG formulation, the approach described in section (2.1) is now reproduced, yielding

$$\frac{\partial u}{\partial t} = \frac{\partial f_v}{\partial x}\,, \quad f_v = \epsilon\, g\,, \tag{40}$$

$$g = \frac{\partial u}{\partial x}\,, \tag{41}$$

such that, in a troubled element Ω, one has, according to Eqs. (19) and (23),

$$J\frac{dc_i}{dt} = -\epsilon\int_\Omega g\frac{\partial \phi_i}{\partial x}\,dx + \left[\tilde{f}_v\phi_i\right]_\ominus^\oplus\,, \tag{42}$$

$$J\gamma_j = -\int_\Omega u\frac{\partial \phi_j}{\partial x}\,dx + \left[\tilde{u}\,\phi_j\right]_\ominus^\oplus\,, \tag{43}$$

whose integrations can be moved to Ω_{st}, so that, recalling Eqs. (4) and (20),

$$J\frac{dc_i}{dt} = \left[\tilde{f}_v\phi_i\right]_\ominus^\oplus - \epsilon\sum_j \gamma_j\mu_{ji}\,, \tag{44}$$

$$J\gamma_j = \left[\tilde{u}\,\phi_j\right]_\ominus^\oplus - \sum_k c_k\mu_{kj}\,, \tag{45}$$

ISSN 2176-5480

where the summations from here on always varies from 0 to P, and μ is defined as

$$\mu_{ab} = \int_{\Omega_{st}} \phi_a \frac{\partial \phi_b}{\partial \xi}\, d\xi \,. \tag{46}$$

Using Eq. (45) into Eq. (44) gives

$$J^2 \frac{dc_i}{dt} = J \left[\tilde{f}_v \phi_i\right]_{\ominus}^{\oplus} - \epsilon \sum_j \mu_{ji} \left\{ [\tilde{u}\, \phi_j]_{\ominus}^{\oplus} - \sum_k c_k \mu_{kj} \right\}, \tag{47}$$

but noting that

$$\sum_j \mu_{ji} \left[\tilde{u}\, \phi_j\right]_{\ominus}^{\oplus} = \tilde{u}^{\oplus} \sum_j \mu_{ji} \phi_j^{\oplus} - \tilde{u}^{\ominus} \sum_j \mu_{ji} \phi_j^{\ominus} = \left[\tilde{u} \sum_j \mu_{ji} \phi_j \right]_{\ominus}^{\oplus}, \tag{48}$$

$$\sum_j \mu_{ji} \left(\sum_k c_k \mu_{kj} \right) = \sum_{j,k} c_k \mu_{kj} \mu_{ji} = \sum_k c_k \left(\sum_j \mu_{kj} \mu_{ji} \right), \tag{49}$$

turns Eq. (47) into

$$J^2 \frac{dc_i}{dt} = J \left[\tilde{f}_v \phi_i\right]_{\ominus}^{\oplus} - \epsilon \left[\tilde{u} \sum_j \mu_{ji} \phi_j \right]_{\ominus}^{\oplus} + \epsilon \sum_k c_k \left(\sum_j \mu_{kj} \mu_{ji} \right), \tag{50}$$

which can be seen as an ODE system, where the first two terms on the right-hand side contain the boundary conditions for the diffusion PDE and the third term is a linear combination of the coefficients c_i.

3.2 On the local boundary conditions

An important characteristic of a limiter is the conservativity property, which in the context of high-order methods means that the average value of the numerical solution within a troubled element must remain unchanged during the limiting process. When dealing with a modal DG formulation, it is sufficient to keep untouched the first coefficient of the local expansion, since

$$\int_\Omega u\, dx = \frac{1}{\phi_0} \int_\Omega \phi_0 \sum_i c_i \phi_i\, dx = \frac{J c_0}{\phi_0} \,. \tag{51}$$

Now, noting from Eq. (46) that $\mu_{j0} = 0 \;\forall\; j$, Eq. (50) yields

$$J \frac{dc_0}{dt} = \left[\tilde{f}_v \phi_0\right]_{\ominus}^{\oplus} = \tilde{f}_v^{\oplus} \phi_0^{\oplus} - \tilde{f}_v^{\ominus} \phi_0^{\ominus} = \left(\tilde{f}_v^{\oplus} - \tilde{f}_v^{\ominus} \right) \phi_0 \,, \tag{52}$$

so that exact conservativity would require $\tilde{f}_v^{\oplus} = \tilde{f}_v^{\ominus} = 0$. This, however, is not an option because of stability issues. More specifically, the ODE in Eq. (50) can be verified to be unstable when such condition is adopted. Despite of this, conservativity can still be pursued in a weaker sense.

In the following analysis, the letters R and L will be used to denote properties outside the troubled element, referring to properties of virtual elements at the right (R) and left (L) sides of the troubled element. For now, the central element should be regarded as disconnected from the global mesh and from its real neighboring elements. In what follows, the (local) boundary conditions used for the solution of Eq. (50) within a troubled element will be discussed.

Using Eqs. (29) to (33), one can write

$$\tilde{f}_v^{\oplus} = \frac{1}{2} \left\{ \frac{\epsilon}{J} \sum_i c_i \partial_\xi \phi_i^{\oplus} + \epsilon_R \left[\frac{\partial u}{\partial x} \right]_R + \frac{\eta}{2} \left(u_R - \sum_i c_i \phi_i^{\oplus} \right) \sum_i \left[\frac{\epsilon}{J} \left(\phi_i^{\oplus} \right)^2 + \frac{\epsilon_R}{J_R} \left(\phi_i^{\ominus} \right)^2 \right] \right\}, \tag{53}$$

$$\tilde{f}_v^{\ominus} = \frac{1}{2} \left\{ \epsilon_L \left[\frac{\partial u}{\partial x} \right]_L + \frac{\epsilon}{J} \sum_i c_i \partial_\xi \phi_i^{\ominus} + \frac{\eta}{2} \left(\sum_i c_i \phi_i^{\ominus} - u_L \right) \sum_i \left[\frac{\epsilon_L}{J_L} \left(\phi_i^{\oplus} \right)^2 + \frac{\epsilon}{J} \left(\phi_i^{\ominus} \right)^2 \right] \right\}. \tag{54}$$

Since the whole expressions of $\tilde{f}_v^{\oplus}$ or $\tilde{f}_v^{\ominus}$ cannot be made zero, a first idea in that direction would be to prescribe values for $[\partial u/\partial x]_R$ and $[\partial u/\partial x]_L$ such that

$$\frac{\epsilon}{J} \sum_i c_i \partial_\xi \phi_i^{\oplus} + \epsilon_R \left[\frac{\partial u}{\partial x} \right]_R = \epsilon_L \left[\frac{\partial u}{\partial x} \right]_L + \frac{\epsilon}{J} \sum_i c_i \partial_\xi \phi_i^{\ominus} = 0 \,, \tag{55}$$

ISSN 2176-5480

by which the numerical viscous fluxes would become

$$\tilde{f}_v^{\oplus} = \frac{\eta}{4}\left(u_R - \sum_i c_i \phi_i^{\oplus}\right) \sum_i \left[\frac{\epsilon}{J}\left(\phi_i^{\oplus}\right)^2 + \frac{\epsilon_R}{J_R}\left(\phi_i^{\ominus}\right)^2\right], \tag{56}$$

$$\tilde{f}_v^{\ominus} = \frac{\eta}{4}\left(\sum_i c_i \phi_i^{\ominus} - u_L\right) \sum_i \left[\frac{\epsilon_L}{J_L}\left(\phi_i^{\oplus}\right)^2 + \frac{\epsilon}{J}\left(\phi_i^{\ominus}\right)^2\right]. \tag{57}$$

At this point, one must note that if u_R and u_L were calculated as a composition of the solution values at the interfaces of the real mesh, i.e. taking into account the global solution, than the property jumps (the first expressions in parenthesis above) would be of magnitude $O(h/p)$, since that is the error level of the global solution in the vicinity of shocks, as discussed in section (2.2). Following this approach, the error introduced by the limiter in the solution average value, obtained by the variation Δc_0, recall Eq. (52), would also be of magnitude $O(h/p)$. For the sake of consistency, this would also guarantee that $\Delta c_0 \to 0$ through h or p refinement. Therefore, the limiting technique here proposed can be considered conservative within the order of accuracy of the formulation near shocks.

Whatever might be the definitions of u_R and u_L, the values of $\tilde{u}$ needed in Eq. (50) must be prescribed coherently:

$$\tilde{u}^{\oplus} = \frac{1}{2}\left(\sum_i c_i \phi_i^{\oplus} + u_R\right), \tag{58}$$

$$\tilde{u}^{\ominus} = \frac{1}{2}\left(u_L + \sum_i c_i \phi_i^{\ominus}\right). \tag{59}$$

Different formulas for u_R and u_L were tested, but the best results were obtained with a "crossed averaging", namely,

$$u_R = \frac{1}{|S| + |S^R|}\left(|S| \sum_i c_i^R \phi_i^{\ominus} + |S^R| \sum_i c_i \phi_i^{\oplus}\right), \tag{60}$$

$$u_L = \frac{1}{|S^L| + |S|}\left(|S^L| \sum_i c_i \phi_i^{\ominus} + |S| \sum_i c_i^L \phi_i^{\oplus}\right), \tag{61}$$

where c_i, c_i^R and c_i^L are the coefficients of the solution expansion in the troubled element and in its (real) neighbors, the same being true for S, S^R and S^L. Here, S stands for an estimate of the solution slope within the considered elements, given by the second expansion coefficients in a modal DG context, i.e. $S = c_1$, $S^R = c_1^R$ and $S^L = c_1^L$. The idea is that the local boundary conditions should be obtained mainly from outside the troubled element, so as to avoid the use of "noisy data".

3.3 Solving the diffusion ODE

Using Eqs. (56) to (59) into Eq. (50), one can arrive at

$$\frac{2J^2}{\epsilon}\frac{dc_i}{dt} = \sum_j \mu_{ji}\left(u_L \phi_j^{\ominus} - u_R \phi_j^{\oplus}\right) + \frac{\eta\,\zeta}{2}\left(u_L \phi_i^{\ominus} + u_R \phi_i^{\oplus}\right) + \\ + \sum_k c_k \left[\sum_j \mu_{ji}\left(\mu_{kj} - \mu_{jk}\right) - \frac{\eta\,\zeta}{2}\left(\phi_i^{\ominus}\phi_k^{\ominus} + \phi_i^{\oplus}\phi_k^{\oplus}\right)\right], \tag{62}$$

where the variable ζ was defined by the approximations

$$\zeta = \sum_k \left[\left(\phi_k^{\oplus}\right)^2 + \left(\phi_k^{\ominus}\right)^2\right] \cong \sum_k \left[\left(\phi_k^{\oplus}\right)^2 + \frac{J}{J_R}\frac{\epsilon_R}{\epsilon}\left(\phi_k^{\ominus}\right)^2\right] \cong \sum_k \left[\frac{J}{J_L}\frac{\epsilon_L}{\epsilon}\left(\phi_k^{\oplus}\right)^2 + \left(\phi_k^{\ominus}\right)^2\right], \tag{63}$$

which can be done by referring again to the concept of virtual adjacent elements, so that J_L, J_R, ϵ_L and ϵ_R may be defined suitably.

The ODE system given in Eq. (62) is now written in vector form, namely,

$$\frac{2J^2}{\epsilon}\frac{d\mathbf{c}}{dt} = \mathbf{A}\mathbf{c} + \mathbf{b}, \tag{64}$$

ISSN 2176-5480

where $\mathbf{c}$ is the coefficients vector, $\mathbf{A}$ is the system matrix and $\mathbf{b}$ is a vector containing the edge conditions u_L and u_R. Both $\mathbf{A}$ and $\mathbf{b}$ are constants for the local ODE, being given by

$$(\mathbf{A})_{m,n} = \sum_j \mu_{jm} \left(\mu_{nj} - \mu_{jn}\right) - \frac{\eta\,\zeta}{2} \left(\phi_m^{\ominus}\phi_n^{\ominus} + \phi_m^{\oplus}\phi_n^{\oplus}\right) , \tag{65}$$

$$(\mathbf{b})_m = \left(\frac{\eta\,\zeta}{2}\phi_m^{\ominus} + \sum_j \mu_{jm}\phi_j^{\ominus}\right) u_L + \left(\frac{\eta\,\zeta}{2}\phi_m^{\oplus} - \sum_j \mu_{jm}\phi_j^{\oplus}\right) u_R \, . \tag{66}$$

Since matrix $\mathbf{A}$ can be verified to be diagonalizable, an analytical solution for the considered ODE is available. Let $\mathbf{D} = \{...\mathbf{v}_n...\}$ be a matrix whose columns are the (right) eigenvectors of $\mathbf{A}$, and λ_n the respective eigenvalues, such that $\mathbf{A}\mathbf{v}_n = \lambda_n \mathbf{v}_n$. Then, the solution $\mathbf{c}(t)$ can be shown to be

$$\mathbf{c}(t) = \mathbf{D}\mathbf{E}_{\mathbf{c}}\mathbf{D}^{-1}\mathbf{c}_0 + \mathbf{D}\mathbf{E}_{\mathbf{b}}\mathbf{D}^{-1}\mathbf{b} \, , \tag{67}$$

where $\mathbf{c}_0 = \mathbf{c}(t=0)$, while $\mathbf{E}_{\mathbf{c}}$ and $\mathbf{E}_{\mathbf{b}}$ are diagonal time-dependent matrices, given by

$$(\mathbf{E}_{\mathbf{c}})_{n,n} = \exp\left(\lambda_n \frac{\epsilon\, t}{2J^2}\right) , \tag{68}$$

$$(\mathbf{E}_{\mathbf{b}})_{n,n} = \frac{1}{\lambda_n} \exp\left(\lambda_n \frac{\epsilon\, t}{2J^2}\right) - \frac{1}{\lambda_n} \, . \tag{69}$$

3.4 Implementation details

The diffusion-based limiter acts through the operator given in Eq. (67). The limiting should be performed between each step the time-marching process, but only at troubled elements. The oscillating solution is introduced as $\mathbf{c}_0$ and the limited solution is obtained as $\mathbf{c}(t)$, where the duration of the diffusion process must be consistent with the time step used for the time discretization of the original equation, i.e. $t = \Delta t$.

It is important to remind that, for purely hyperbolic problems, the local time step Δt can be calculated directly by Eq. (37). Since the artificial diffusion PDE is not accounted by the DG discretization, but solved analytically, there is no need to use the viscous factor given in Eq. (38). For the same reason, one does not have to worry about employing specific techniques, such as the BR2 scheme, for the discretization of artificial viscosity terms.

One can note by Eq. (65) that the matrix $\mathbf{A}$ is not mesh-dependent, the same being true for its eigenvalues and eigenvectors. Therefore, when applying Eq. (67), one needs only to adjust the diagonal matrices $\mathbf{E}_{\mathbf{c}}$ and $\mathbf{E}_{\mathbf{b}}$ (with the local values of J, ϵ and Δt), and to evaluate the vector $\mathbf{b}$ using the formulas for u_L and u_R given in Eqs. (60) and (61). For each element, the viscosity magnitude ϵ can be obtained by the smooth switching given in Eq. (36).

4. NUMERICAL RESULTS

4.1 Accessing the local accuracy

In order to address the accuracy of the solution (with limiting) in the vicinity of shocks, the inviscid Burgers' equation, given by

$$\frac{\partial u}{\partial t} + \frac{\partial f}{\partial x} = 0 \, , \quad f = \frac{u^2}{2} \, , \tag{70}$$

is here solved for $x \in (-\infty, +\infty)$ with the initial conditions

$$u = \begin{cases} 1 & \text{if } x < -1 \, , \\ -x & \text{if } -1 \leq x \leq 1 \, , \\ -1 & \text{if } x > 1 \, . \end{cases} \tag{71}$$

The exact solution reaches a steady state for $t = 1$, in which $u = -x/|x|$ everywhere except at $x = 0$, where the shock takes place.

For the numerical solution, two spatial discretizations are considered. First, the domain is divided into an odd number of elements to simulate a shock forming in the middle of an element. After that, the domain is divided into an even number of elements to test the case in which the shock forms at the interface between adjacent elements. Full residue convergence was achieved for all cases addressed. The error between exact and numerical solutions is measured in the $L1$ norm.

ISSN 2176-5480

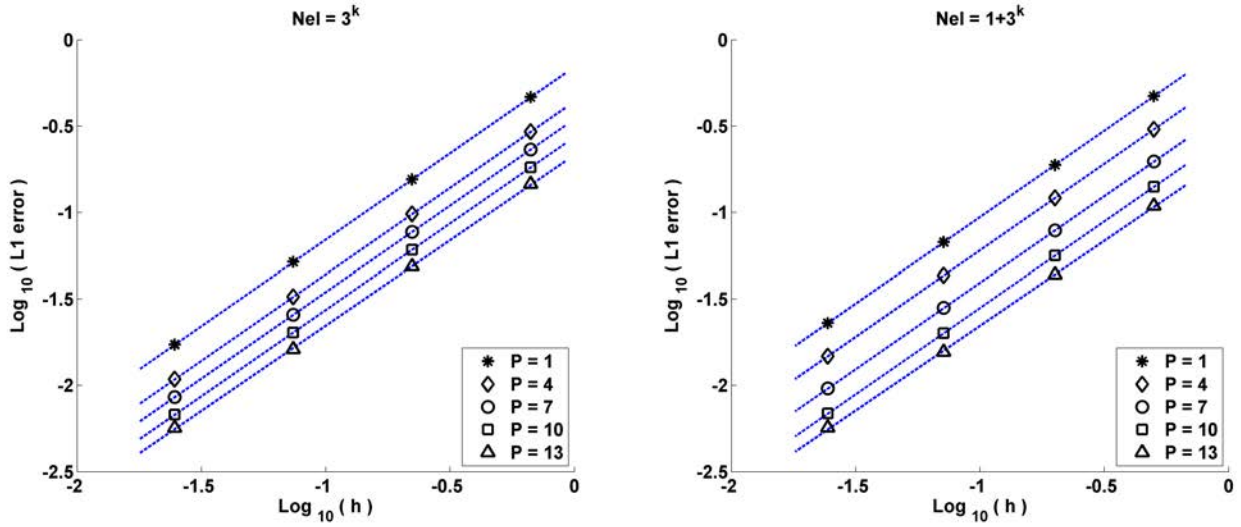

Figure 1. Error convergence for h refinement with different values of P. Slopes equal to 1 were verified for all cases.

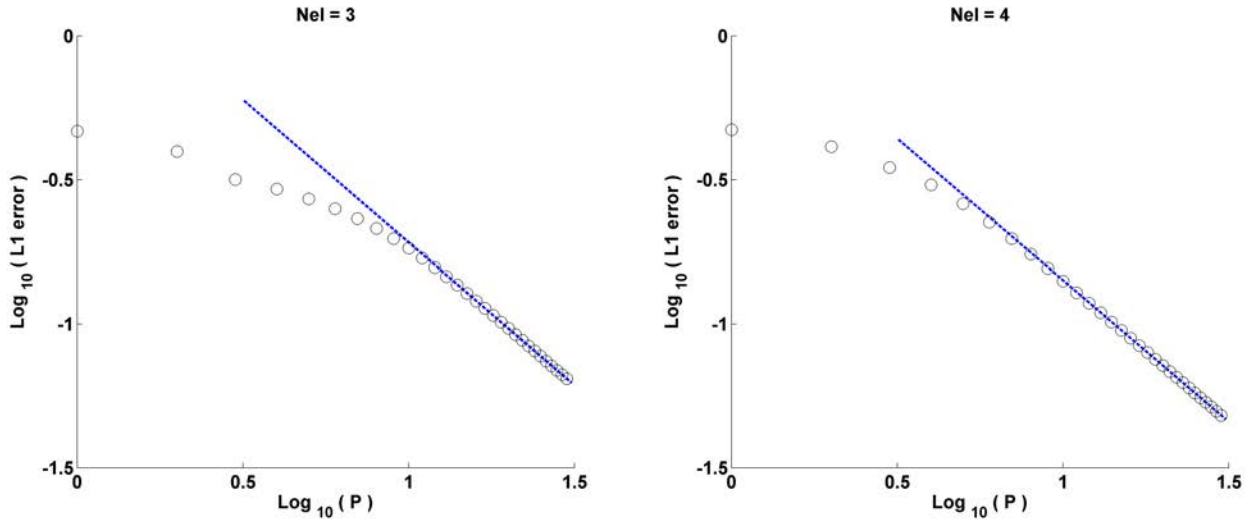

Figure 2. Error convergence for P refinement. Asymptotic slopes equal to -1 were verified.

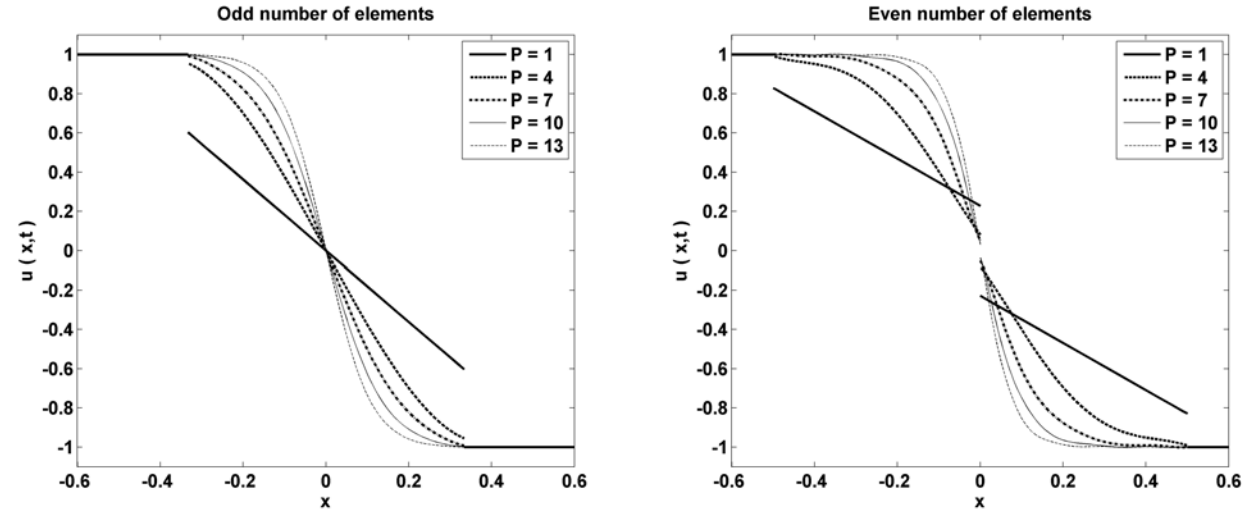

Figure 3. Steady-state shock profiles obtained with different values of P. At the left side, the transition takes place in the middle of an element; at the right side, the shock forms at the interface between adjacent elements.

ISSN 2176-5480

The results obtained for h refinement are given in Fig. 1. Different values of P were tested. For all the cases, the error is shown to decay with h^1, but the actual error level was verified to decrease with increasing P. Such results hold for odd and even number of elements, as can be seen at the left and right sides of Fig. 1, respectively.

The effect of P refinement was then analyzed, and the results are displayed in Fig. 2. The error behavior is again considered for an odd number of elements (such that 3 elements of the same size rely within $[-1, 1]$) as well as for an even number (such that 4 elements of the same size rely within $[-1, 1]$). For both cases, the error is shown to decay asymptotically with p^{-1}.

In summary, the order of accuracy of the numerical solution after limiting is verified to be of magnitude $O(h/p)$ in the vicinity of shocks. The transition profiles obtained at $x = 0$ are shown in Fig. 3 for different values of P. As one can see, fine shock layers are in fact given by the limiting technique here proposed. Solution continuity at interfaces can be more strongly enforced with a higher value of η. For the simulations here considered, the value $\eta = 3$ was used.

4.2 The case of systems

Having fluid flow problems in mind, a modification of the one-dimensional Euler equations in is now considered. The modification consists in the inclusion of a source term to account for flows with area variations, such as those inside ducts or nozzles (Toro, 1999). In conservation form, this model equation can be written as

$$\frac{\partial \mathbf{U}}{\partial t} + \frac{\partial \mathbf{F}}{\partial x} = \mathbf{S} \,, \tag{72}$$

where the vector of conserved variables $\mathbf{U}$, the flux vector $\mathbf{F}$ and the source term $\mathbf{S}$ are given by

$$\mathbf{U} = \{\rho, \rho u, e\}^T \,, \tag{73}$$

$$\mathbf{F} = \left\{\rho u, \rho u^2 + p, (e + p)u\right\}^T \,, \tag{74}$$

$$\mathbf{S} = -d(\ln A)/dx \left\{\rho u, \rho u^2, (e + p)u\right\}^T \,, \tag{75}$$

where $\{\cdot\}^T$ indicates the transpose of a vector, ρ stands for density, u is the velocity, $e = \rho(e_i + u^2/2)$ is the total energy per unit volume, and e_i is the specific internal energy. The static pressure p is obtained using the equation of state for a perfect gas, namely, $p = \rho(\gamma - 1)e_i$, where γ is the fluid ratio of specific heats, which assumes the value $\gamma = 7/5$ for the air. Moreover, the cross-sectional area of the nozzle is denoted by $A = A(x)$.

When applying the diffusion-based limiter to systems, each equation should be treated separately, as if they were independent scalar equations. For instance, in order to evaluate the vector $\mathbf{b}$ in Eq. (67), the values of u_L and u_R must be obtained for each conserved variable of $\mathbf{U}$. The slope factors used in Eqs. (60) and (61) can however be based on an unique characteristic property. Here, the coefficients of the density expansion are used as slope factors.

For the detection of troubled elements, the sensor σ discussed in section 2.2 was applied. In the case of systems, one need to choose a scalar variable upon which the sensor must rely. Here, the element-wise Mach number expansion was used, where the Mach number is given by $M = |u|/a$, being $a = \sqrt{\gamma\, p/\rho}$ the speed of sound. As noted in the work of Huerta *et al.* (2012), this choice grants better results than those obtained when density or entropy expansions are employed.

The considered problem was solved for $x \in [0, 1]$, being the area function prescribed as $A = 0.05 + 1.4(x - 0.5)^2$. Suited boundary conditions were adjusted so that the ratio between the pressure p_e at the exit of the nozzle and the stagnation pressure p_0 at the inflow boundary was fixed as $p_e/p_0 = 7/10$. The domain was discretized into 100 elements of equal size and the solutions obtained with $P = 1$ and $P = 5$ are respectively shown in Figs. 4 and 5. Both figures display the distributions of Mach number and static pressure inside the nozzle, along with the residue convergence history and the limiting-related normalized artificial viscosity ϵ/ϵ_0, recall Eq. (36).

5. CONCLUDING REMARKS

This article presented a new type of shock capturing operator for the Discontinuous Galerkin (DG) method. The DG formulation for convection-diffusion problems was discussed and then a diffusion-based limiter was introduced in a detailed manner. The limiter here proposed works as a filter damping high-frequency modes, but is based on the concept of artificial viscosity. In terms of implementation, the limiting technique is simple, relatively inexpensive, and yet capable of providing results of surprising quality.

Numerical tests demonstrated fine sub-cell resolution as well as local accuracy scaling with h/p (where h is the local mesh size and p is the degree of the polynomial expansion representing the solution). It was also verified that the limiting procedure does not affect the (explicit) time-marching stability envelope nor hinders residue convergence. Such characteristics are specially desired when simulating purely hyperbolic problems with explicit time-stepping.

ISSN 2176-5480

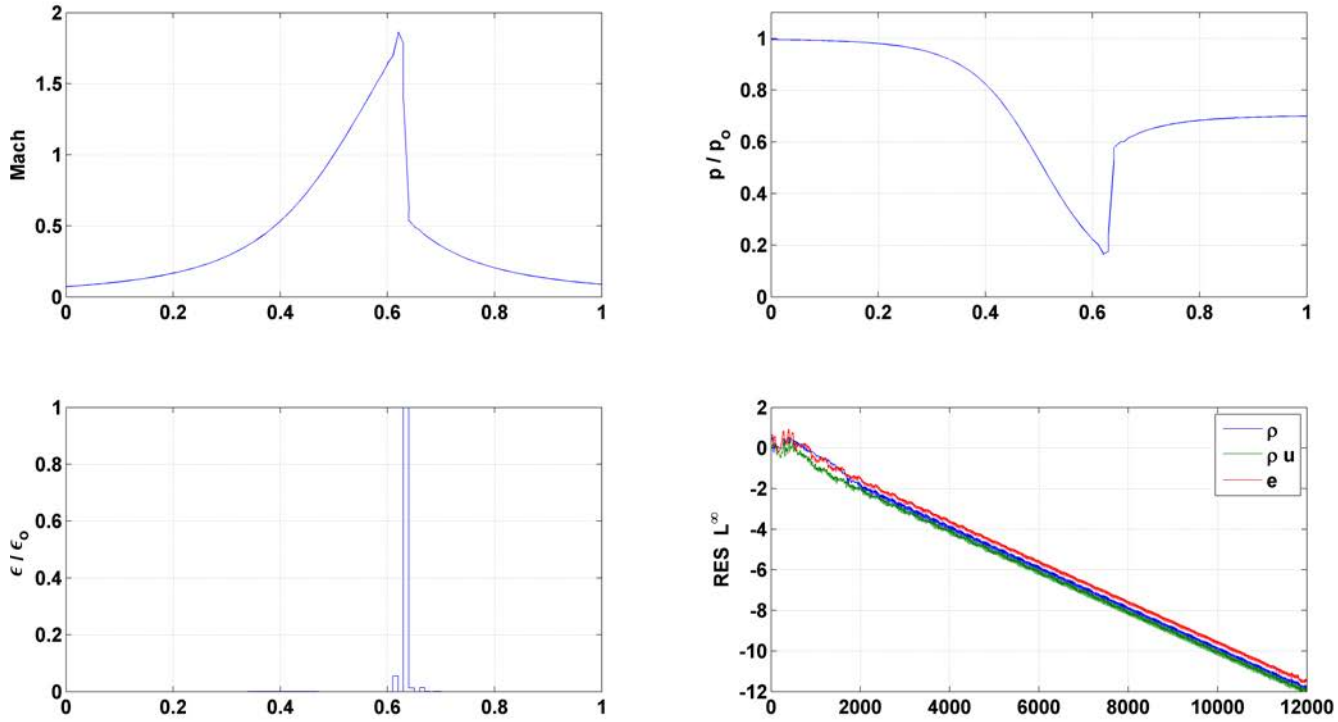

Figure 4. Numerical solution obtained with $P = 1$ for the compressible flow inside a nozzle. The mesh consists of 100 elements of equal size. As one can see, full convergence can be achieved with the diffusion-based limiter.

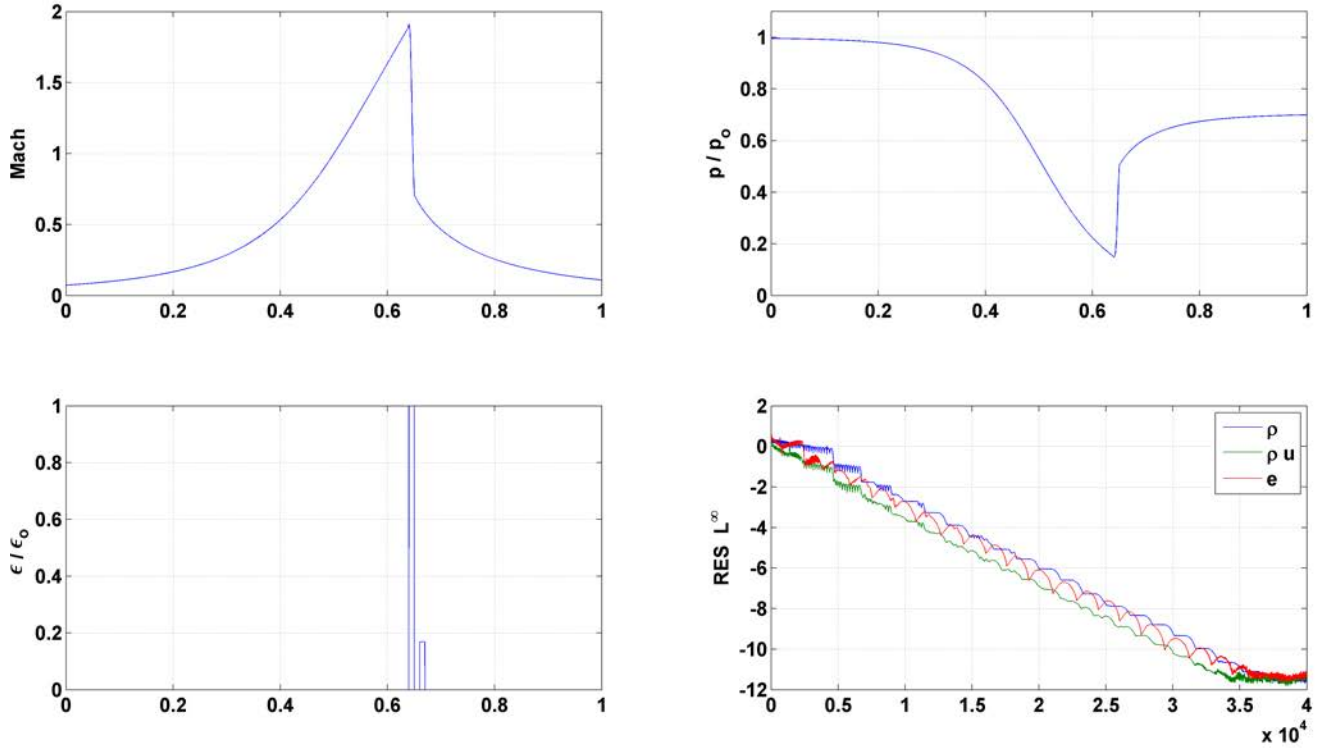

Figure 5. Numerical solution obtained with $P = 5$ for the compressible flow inside a nozzle. The mesh consists of 100 elements of equal size. As one can see, full convergence can be achieved with the diffusion-based limiter.

ISSN 2176-5480

Among future research possibilities, one can mention the development of better suited, parameter-free, oscillation sensors for the detection of troubled elements, the analysis of different averaging formulas for the limiting-related local boundary conditions and, of course, the extension of the diffusion based-limiter for fluid flow equations in two and three dimensions.

6. ACKNOWLEDGEMENTS

The authors gratefully acknowledge the support for this research provided by FAPESP (Sao Paulo Research Foundation), under the Research Grant No. 2012/16973-5.

7. REFERENCES

Anderson, J.D., 2002. *Modern Compressible Flow: With Historical Perspective*. McGraw-Hill, New York, 3rd edition.

Arnold, D.N., Brezzi, F., Cockburn, B. and Marini, L.D., 2002. "Unified analysis of discontinuous Galerkin methods for elliptic problems". *SIAM Journal on Numerical Analysis*, Vol. 39, No. 5, pp. 1749–1779.

Askey, R., 2005. "The 1839 paper on permutations: its relation to the Rodrigues' formula and further developments". In: Altmann, S. L.; Ortiz, E. L. (Eds.) *Mathematics and social utopias in France: Olinde Rodrigues and his times*. American Mathematical Society.

Atkins, H. and Pampell, A., 2011. "Robust and accurate shock capturing method for high-order discontinuous Galerkin methods". In *Proceedings of the 20th AIAA Computational Fluid Dynamics Conference (AIAA Paper 2011-3058)*. Honolulu, USA.

Barter, G.E. and Darmofal, D.L., 2007. "Shock capturing with higher-order, PDE-based artificial viscosity". In *Proceedings of the 18th AIAA Computational Fluid Dynamics Conference (AIAA Paper 2007-3823)*. Miami, USA.

Barter, G.E. and Darmofal, D.L., 2010. "Shock capturing with PDE-based artificial viscosity for DGFEM: Part I. Formulation". *Journal of Computational Physics*, Vol. 229, pp. 1810–1827.

Bassi, F., Rebay, S., Mariotti, G., Pedinotti, S. and Savini, M., 1997. "A high-order accurate discontinuous finite element method for inviscid and viscous turbomachinery flows". In *Proceedings of the 2nd European Conference on Turbomachinery Fluid Dynamics and Thermodynamics*. Antwerp, Belgium.

Brezzi, F., Manzini, G., Marini, L.D., Pietra, P. and Russo, A., 2000. "Discontinuous Galerkin approximations for elliptic problems". *Numerical Methods for Partial Differential Equations*, Vol. 16, pp. 365–378.

Cockburn, B., Karniadakis, G.E. and Shu, C.W., 2000. "The development of discontinuous Galerkin methods". In: Cockburn, B.; Karniadakis, G.E.; Shu, C.W. (Eds.) *Discontinuous Galerkin methods: theory, computation and applications*. Springer, Berlin.

Cockburn, B. and Shu, C.W., 2001. "Runge-Kutta discontinuous Galerkin methods for convection-dominated problems". *SIAM Journal of Scientific Computing*, Vol. 16, No. 3, pp. 173–261.

Ekaterinaris, J.A., 2005. "High-order accurate, low numerical diffusion methods for aerodynamics". *Progress in Aerospace Sciences*, Vol. 41, pp. 192–300.

Hesthaven, J.S. and Warburton, T., 2008. *Nodal discontinuous Galerkin methods: algorithms, analysis and applications*. Springer, New York.

Huerta, A., Casoni, E. and Peraire, J., 2012. "A simple shock-capturing technique for high-order discontinuous Galerkin methods". *International Journal for Numerical Methods in Fluids*, Vol. 69, pp. 1614–1632.

Johnson, C. and Pitkaranta, J., 1986. "An analysis of the discontinuous Galerkin method for a scalar hyperbolic equation". *Mathematics of Computation*, Vol. 43, pp. 1–26.

Karniadakis, G.E. and Sherwin, S.J., 2005. *Spectral/hp element methods for computational fluid dynamics*. Oxford University Press, Oxford, 2nd edition.

Klockner, A., Warburton, T. and Hesthaven, J.S., 2011. "Viscous shock capturing in a time-explicit discontinuous Galerkin method". *Mathematical Modeling of Natural Phenomena*, Vol. 10, pp. 1–27.

Krivodonova, L., 2007. "Limiters for high-order discontinuous Galerkin methods". *Journal of Computational Physics*, Vol. 226, pp. 879–896.

Kuzmin, D., 2010. "A vertex-based hierarchical slope limiter for p-adaptive discontinuous Galerkin methods". *Journal of Computational and Applied Mathematics*, Vol. 233, pp. 3077–3085.

Lê, T.H., Le Gouez, J.M. and Garnier, E., 2011. "High accuracy flow simulations: Advances and challenges for future needs in aeronautics". *Computers & Fluids*, Vol. 43, pp. 90–97.

Moura, R.C., 2012. *A High-Order Unstructured Discontinuous Galerkin Finite Element Method for Aerodynamics*. Master's thesis, Instituto Tecnológico de Aeronáutica, São José dos Campos.

Nogueira, A.C., Cantão, R.F., Silva, C.A.C. and Bigarella, E.D.V., 2010. "Development of a commercial CFD tool based on a discontinuous Galerkin formulation". In *Proceedings of the 28th AIAA Applied Aerodynamics Conference (AIAA Paper 2010-5075)*. Chicago, USA.

Persson, P.O. and Peraire, J., 2006. "Sub-cell shock capturing for discontinuous Galerkin methods". In *Proceedings of*

ISSN 2176-5480

the 44th AIAA Aerospace Sciences Meeting and Exhibit (AIAA Paper 2006-112). Reno, USA.

Qiu, J. and Shu, C.W., 2005. "Runge-Kutta discontinuous Galerkin using WENO limiters". *SIAM Journal of Scientific Computing*, Vol. 26, No. 3, pp. 907–929.

Richter, G.R., 1992. "The discontinuous Galerkin method with diffusion". *Mathematics of Computation*, Vol. 58, pp. 631–643.

Rider, W.J. and Lowrie, R.B., 2002. "The use of classical Lax-Friedrichs Riemann solvers with discontinuous Galerkin methods". *International Journal for Numerical Methods in Fluids*, Vol. 40, pp. 479–486.

Toro, E.F., 1999. *Riemann solvers and numerical methods for fluid dynamics - a practical introduction*. Springer, Berlin.

Toulorge, T. and Desmet, W., 2011. "CFL conditions for Runge-Kutta discontinuous Galerkin methods on triangular grids". *Journal of Computational Physics*, Vol. 230, pp. 4657–4678.

Vincent, P.E. and Jameson, A., 2011. "Facilitating the adoption of unstructured high-order methods amongst a wider community of fluid dynamicists". *Mathematical Modeling of Natural Phenomena*, Vol. 6, No. 3, pp. 97–140.

von Neumann, J. and Richtmyer, R.D., 1950. "A method for the numerical calculation of hydrodynamic shocks". *Journal of Applied Physics*, Vol. 21, pp. 232–237.

Wang, Z.J., 2007. "High-order methods for the Euler and Navier-Stokes equations on unstructured grids". *Progress in Aerospace Sciences*, Vol. 43, pp. 1–41.

Wang, Z.J., Fidkowski, K., Abgrall, R., Bassi, F., Caraeni, D., Cary, A., Deconinck, H., Hartmann, R., Hillewaert, K., Huynh, H.T., Kroll, N., May, G., Persson, P.O., van Leer, B. and Visbal, M., 2013. "High-order CFD methods: current status and perspective". *International Journal for Numerical Methods in Fluids*. Available online (DOI: 10.1002/fld.3767).

Wu, C., Deng, J. and Chen, F., 2008. "Diffusion Equations over Arbitraty Triangulated Surfaces for Filtering and Texture Applications". *IEEE Transactions on Visualization and Computer Graphics*, Vol. 14, No. 3, pp. 666–679.

8. RESPONSIBILITY NOTICE

The authors are the only responsible for the printed material included in this paper.